Chemical Engineering Journal 157 (2010) 238–248

Contents lists available at ScienceDirect

Chemical Engineering Journal

journal homepage: www.elsevier.com/locate/cej

Removal of cadmium from aqueous solutions by oxidized and ethylenediamine-functionalized multi-walled carbon nanotubes

Goran D. Vuković[a], Aleksandar D. Marinković[a], Miodrag Čolić[b], Mirjana Đ. Ristić[a], Radoslav Aleksić[a], Aleksandra A. Perić-Grujić[a], Petar S. Uskoković[a,*]

[a] Faculty of Technology and Metallurgy, University of Belgrade, Karnegijeva 4, 11120 Belgrade, Serbia
[b] Institute for Medical Research, Military Medical Academy, Crnotravska 17, 11002 Belgrade, Serbia

ARTICLE INFO

Article history:
Received 10 July 2009
Received in revised form
13 November 2009
Accepted 22 November 2009

Keywords:
Cadmium adsorption
Carbon nanotubes
Amino-functionalization
Cytotoxicity

ABSTRACT

Surface functionalization of multi-walled carbon nanotubes (MWCNTs) by ethylenediamine, *via* chemical modification of carboxyl groups, using O-(7-azabenzotriazol-1-yl)-N,N,N′,N′-tetramethyluronium hexafluorophosphate, was performed. The resulting materials were characterized by different techniques, such as FTIR, TGA and elemental analysis. Biocompatibility studies showed that the functionalized MWCNTs, at concentrations between 1 and 50 $\mu g\,mL^{-1}$, were not cytotoxic for the fibroblast L929 cell line. In batch tests, the influences of solution pH, contact time, initial metal ion concentration and temperature on the sorption of Cd^{2+} ions onto raw-MWCNTs (raw-MWCNT), oxidized MWCNTs (o-MWCNT) and ethylenediamine-functionalized MWCNTs (e-MWCNT) were studied. The adsorption of Cd^{2+} ions by o-MWCNT and e-MWCNT was strongly pH dependent. The time dependent Cd^{2+} sorption onto raw-MWCNT, o-MWCNT and e-MWCNT can be described by a pseudo-second-order kinetic model. The Langmuir isotherm model agrees well with the equilibrium experimental data. The maximum capacity was obtained for e-MWCNT, 25.7 $mg\,g^{-1}$, at 45 °C. The thermodynamic parameters were also deduced for the adsorption of Cd^{2+} ions on raw-MWCNT, o-MWCNT and e-MWCNT and the results showed that the adsorption was spontaneous and endothermic.

1. Introduction

Carbon nanotubes (CNTs) are relatively new materials with an increasing number of applications due to their unique electrical, mechanical, optical and chemical properties [1,2]. These excellent properties make CNTs promising materials for numerous applications, such as hydrogen storage [3], catalyst supports [4], chemical sensors [5] and nanoelectronic devices [6]. Since it has been proven that CNTs possess potential for the removal of many kinds of pollutants from water because of their ability to establish π–π electrostatic interactions and their large surface areas, CNTs have attracted great attention in analytical chemistry and environmental protection [7,8]. CNTs have shown exceptional adsorption capabilities and high adsorption efficiencies for various organic pollutants, such as aniline, phenol and their substitutes [9], as well as diazinon [10]. In addition, CNTs were found to be superior sorbents for several divalent metal ions [8,11–16].

However, the application of CNTs has been largely hampered by their poor dispersion into solvents, due to the strong intermolecular van der Waals interactions between the tubes, which can lead to the formation of aggregates. A common technique to improve dispersion and realize the great capability of CNTs is through chemical functionalization, which is used relatively often to generate functional groups on the surface of CNTs. The covalent side-wall modifications of nanotubes have been well described in several review papers [17,18]. In general, major approaches include: (i) amidation or esterification of carboxylated CNTs, (ii) side-wall covalent attachment of functional groups directly to pristine CNTs. Modification of the surface morphology plays an important role in enhancing the sorption capacity of CNTs. Activation of CNTs under oxidizing conditions with chemicals such as HNO_3, $KMnO_4$, H_2O_2, NaOCl, H_2SO_4, KOH, and NaOH have been widely reported [8–16]. During activation, metallic impurities and catalyst support materials are dissolved and the surface characteristics are altered due to the introduction of new functional groups (*e.g.*, COOH, OH, C=O, OSO_3H, lactones) [8–16]. Many other functional groups could also be appropriate for metal ion sorption. Due to their high reactivity with many chemical species, it has been suggested that amino groups together with oxygen groups could serve as coordination and electrostatic interaction sites for transition metal sorption [19–23].

The practical use of CNTs as sorbents in water and wastewater treatment is limited due to the toxicity of CNTs and CNT-related

* Corresponding author. Tel.: +381 11 3303 831; fax: +381 11 3370 387.
E-mail address: puskokovic@tmf.bg.ac.rs (P.S. Uskoković).

1385-8947/$ – see front matter © 2009 Elsevier B.V. All rights reserved.
doi:10.1016/j.cej.2009.11.026

materials. Toxicological investigations and identification of compounds that could interact with animals and humans is of utmost importance. Several CNT biocompatibility and cytotoxicity studies have been performed in recent years [24–28], but it is not clear if the cytotoxicity is due to the CNTs themselves or to their contaminants, such as metallic catalysts or amorphous carbon structures. Clearly, in the studies that obtained good cell viability, some kind of purification or functionalization of CNTs was performed [25,27]. Although functionalization of CNTs results in significant reduction of their cytotoxicity and improved biocompatibility [25], little is known whether and how the functional groups or molecules modify cellular response to CNTs.

In this study, the possibility of the employment of amino-functionalized multi-walled carbon nanotubes (MWCNTs) as a sorbent for the removal of Cd^{2+} ions from aqueous solutions was examined. Modification of the material was realized according to our previous study [29], in which MWCNTs were functionalized by 1,6-hexanediamine, diethylenetriamine, triethylenetetramine and 1,4-phenylenediamine. In this study, the direct coupling of ethylenediamine (EDA) with carboxylic groups to introduce amino groups *via* amide formation using O-(7-azabenzotriazol-1-yl)-N,N,N′,N′-tetramethyluronium hexafluorophosphate (N-HATU) was performed. This reaction is important because common acylation-amidation chemistry requires reaction times of about 3–5 days and high reaction temperatures [30]. A detailed characterization of the MWCNTs was performed using a variety of techniques such as FTIR, TGA and elemental analysis. The biocompatibility of the EDA-functionalized (e-MWCNT), oxidized (o-MWCNT) and control pristine MWCNTs (raw-MWCNT) was comparatively studied on the mouse fibroblast cell line, L929.

Cadmium, which is a non-essential metal for humans, has various applications in a variety of industrial processes and operations. It directly reaches water bodies through industrial effluent, causing a marked increase in its concentration. It has toxic effects and causes various types of acute and chronic disorders. Exposure to cadmium may cause nausea, salivation, muscular cramps and anemia, while extended exposure may also cause cancer [11,31].

The goal of this research was to evaluate the sorption behavior of Cd^{2+} onto MWCNTs and to compare the performance of MWCNTs adsorbents with those of other adsorbents. To achieve this goal, the influence of experimental conditions, such as pH value, concentration and temperature, on the sorption behavior was investigated. The adsorption thermodynamics and kinetics were also studied. The sorption of Cd^{2+} ions by raw-MWCNT, o-MWCNT and e-MWCNT were compared.

2. Experimental details

2.1. Materials

MWCNTs prepared by a chemical vapor deposition (CVD) method were used as received without purification. The purity of MWCNTs was more than 95% and the outer and inner diameters were 20–30 and 5–10 nm, respectively and the length between 5 and 200 μm. All other reagents such as EDA, N-HATU, concentrated H_2SO_4 acid, concentrated HNO_3 acid and methanol were used as received. Millipore deionized (DI) water (18 MΩ cm resistance) was used for sample washing and solution preparation. All chemicals and MWCNTs were obtained from Sigma-Aldrich.

Analytical-grade cadmium nitrate standard (Baker) was employed to prepare a stock solution containing 1000 μg mL^{-1} of Cd^{2+}, which was further diluted with DI water to the required Cd^{2+} concentrations for the sorption measurements.

2.2. Material preparation

The raw-MWCNTs were first treated with a (v/v 3:1) mixture of concentrated H_2SO_4 and HNO_3 (Scheme 1). This mixture was then sonicated for 3 h at 40 °C in an ultrasonic bath to introduce oxygen groups onto the MWCNT surface. After cooling to room temperature, the o-MWCNTs were added dropwise to 300 mL of cold DI water and vacuum-filtered through a 0.05 μm pore size PTFE membrane filter. The filtrant was washed with DI water until the pH was neutral. The sample was dried in a vacuum oven at 80 °C for 8 h. The oxidized nanotubes (100 mg) were dispersed in EDA (60 mL). The coupling agent, N-HATU, (8 mg) was added and the dispersion was sonicated for 4 h at 40 °C (Scheme 1). The obtained product was diluted with 300 mL of methanol and vacuum-filtered using a 0.05 μm pore size PTFE membrane filter, after which the filtrant was washed extensively with excess methanol. Thus obtained e-MWCNTs were dried in a vacuum oven at 60 °C for 8 h.

2.3. Characterization of MWCNTs

Fourier-transform infrared (FTIR) spectra were recorded in the transmission mode using a BOMEM (Hartmann & Braun) spectrometer. Thermogravimetric analysis (TGA) was performed using a TA Instruments SDT Q600 from 20 to 800 °C at a heating rate of 20 °C min^{-1} and a nitrogen flow of 200 mL min^{-1}. Elemental analyses were performed using a VARIO EL III Elemental analyser. The BET specific surface area, pore specific volume and pore diameter were measured by nitrogen adsorption/desorption at 77.4 K using a Micromeritics ASAP 2020MP gas sorption analyzer. The pH values at the point of zero charge (pH_{PZC}) of the samples were measured using the pH drift method [14]. The zeta potential measurements of the raw-MWCNT, o-MWCNT and e-MWCNT samples were performed using a Zeta-sizer Nano-ZS equipped with a 633 nm He-Ne laser (Malvern). Suspensions of the samples at a concentration of 100 mg L^{-1} in DI water were sonicated for 5 min and the pH values of the suspensions were measured after the zeta potential measurements. The acidic and basic site concentrations were determined using the Boehm titration method [32].

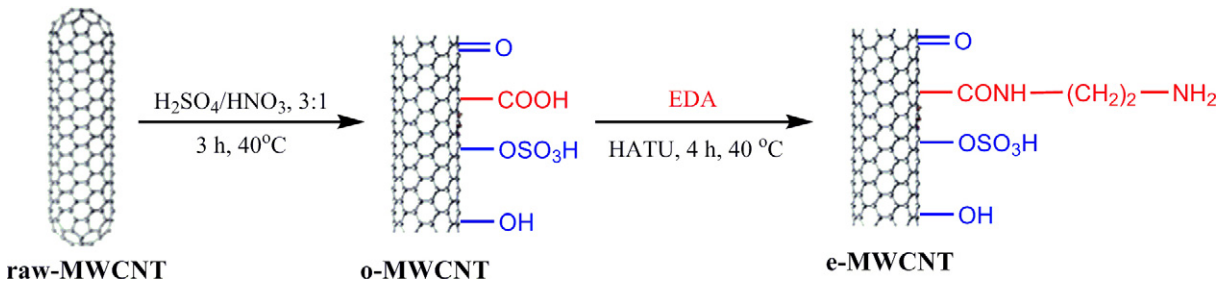

Scheme 1. Schematic presentation of the functionalization of MWCNTs.

2.4. Biocompatibility studies

The biocompatibility of the raw-MWCNT, o-MWCNT and e-MWCNT was studied using the mouse fibroblast cell line L929 as described in our previous study [29]. The cells were cultivated in 24-well plates (2×10^4 cells/well) in RPMI medium (Sigma), supplemented with 5% fetal calf serum (Sigma), 2 mmol L^{-1} L-glutamine and antibiotics for 5 days, using different concentrations of pristine or modified MWCNTs. Prior to dilution in the cell culture medium, aqueous stock solutions of the MWCNTs were sonicated in an ultrasonic bath for 1 h. After 1, 3 or 5 days of cultivation, the cells were trypsinized (0.2% trypsine/EDTA) and counted using 0.2% Trypan Blue. Relative values (%) of the total number of viable cells for each time interval were calculated based on the total number of L929 cells in the control wells without MWCNTs, used as 100%. The relative values of necrotic cells were determined by flow cytometry (EPICS XL/MCL, Coulter), after addition of 40 μg mL^{-1} propidium iodide (PI) (Sigma) to the cells. Apoptosis was measured by flow cytometry after staining the cells with a hypotonic solution of PI, as described elsewhere [24]. The cells with hypodiploid nuclei were considered as apoptotic cells. The effect of MWCNTs on the proliferation activity of L929 cells was determined using a ^{3}[H]-thymidine incorporation assay. Briefly, L929 cells were cultivated in 96-well plates (0.5×10^4 cells/well) with different concentrations of MWCNTs for 48 h. During the last 8 h of cultivation, the cells were pulsed with 1 μCi $well^{-1}$ ^{3}[H]-thymidine (6.7 Ci $mmol^{-1}$, Amersham). After cell trypsinization and harvesting, the radioactivity was counted using a scintillation counter (Beckman). The results are expressed as mean counts per minute (cpm) of triplicate measurements.

2.5. Adsorption experiments

Batch sorption experiments were performed using 10 mL bottles with addition of 1 mg of MWCNTs and 10 mL of Cd^{2+} solution of initial concentrations (C_0) 0.1, 0.5, 1, 3 and 5 mg L^{-1}. The bottles were placed in an ultrasonic bath, which was operated at defined temperatures and times. In order to evaluate the effect of pH on Cd^{2+} adsorption, the initial pH values of the solutions were varied between 2.0 and 11.0 by adjustment with 0.01 and 0.1 mol L^{-1} NaOH and 0.01 and 0.1 mol L^{-1} HNO_3, at 25 °C. The mixtures of MWCNTs and Cd^{2+} solutions were ultrasonically treated for 45 min at 25 °C and then filtered through a 0.2 μm PTFE membrane filter. The adsorption thermodynamic experiments were performed at 25, 35 and 45 °C. The effect of MWCNTs-Cd^{2+} contact time was followed in the range 5–100 min. The amount of adsorbed Cd^{2+} ions was determined by the difference between the initial and the equilibrium concentration. To evaluate the regeneration capacity, MWCNTs after adsorption to equilibrium at an initial Cd^{2+} concentration of 5 mg L^{-1} were dried at 60 °C for 2 h, and then dispersed in DI water of different pH values (from 1.5 to 6), adjusted using 0.1 mol L^{-1} HCl. After the solutions had reached equilibrium, the Cd^{2+} concentrations were remeasured and the desorption results were then obtained. The data analysis was realized using a normalized standard deviation Δq (%) calculated using the following equation:

$$\Delta q(\%) = \sqrt{\sum \frac{[(q_{exp} - q_{cal})/q_{exp}]^2}{N-1}} \times 100 \quad (1)$$

where q_{exp} and q_{cal} are the experimental and calculated amounts of Cd^{2+} adsorbed on the MWCNTs and N is the number of data points. All the experiments were performed in triplicate and only the mean values are reported. The maximum deviation was <3% (experimental error). All calculated (estimated) standard errors of the isotherm, kinetic and thermodynamic parameters were determined by commercial software (Microcal Origin 7.0) with a linear regression program. The results of Cd^{2+} sorption on polyethylene test tube wall and filters showed that Cd^{2+} adsorption on this material was negligible.

Measurements of Cd^{2+} concentrations were realized using an Agilent Technologies 7500ce ICP-MS system (Agilent Technologies, Inc.) equipped with an octopole collision/reaction cell, Agilent 7500 ICP-MS ChemStation software, a MicroMist nebulizer and a Peltier cooled (2 °C) quartz Scott-type double pass spray chamber. The instrument was optimized daily in terms of sensitivity, level of oxide and doubly charged ions using a tuning solution containing 1 μg L^{-1} of Li, Y, Tl, Ce, Co and Mg in 2% HNO_3 (w/v). Standard optimization procedures and criteria specified in the manufacturer's manual were followed. The detection limit of the method was 4.0×10^{-5} mg L^{-1} of Cd^{2+}.

3. Results and discussion

3.1. MWCNTs characterization

The FTIR spectra of raw-MWCNT, o-MWCNT and e-MWCNT are compared in Fig. 1a. The H_2SO_4-HNO_3 treatment produced carboxyl group on the external surface of the MWCNTs due to oxidation, as indicated by the presence of characteristic peaks at ≈3438 and ≈1726 cm^{-1} of the stretching vibrations of ν(OH) and ν(C=O) of the carboxylic groups (COOH), respectively (Fig. 1a) [14,29,33]. The asymmetric and symmetric stretching vibrations $\nu_{as}(CH_2)$ and $\nu_s(CH_2)$ were situated at ≈2924 and ≈2856 cm^{-1}. Overlapped vibrations of double bonds C=C and carbonyl groups C=O were

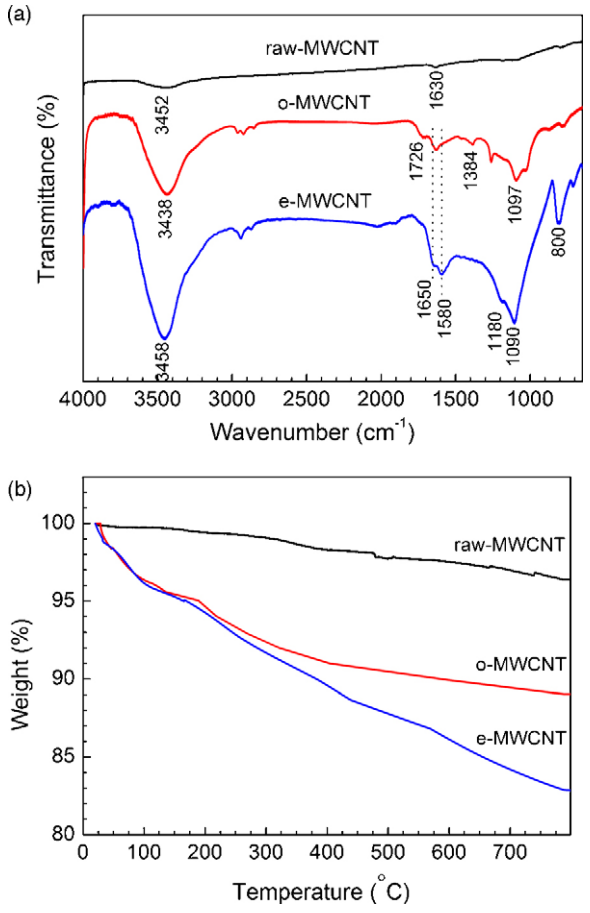

Fig. 1. (a) FTIR transmission spectra and (b) TGA curves of raw-MWCNT, o-MWCNT and e-MWCNT.

Table 1
Elemental analysis of raw-MWCNT, o-MWCNT and e-MWCNT.

Sample	C (%)	H (%)	N (%)	S (%)	O (%)
raw-MWCNT	97.46	0.32	0	0	2.22
o-MWCNT	82.13	1.18	0.49	0.64	15.56
e-MWCNT	80.08	1.76	4.08	0.58	13.50

present at ≈1631 cm^{-1}. The peak at ≈1384 cm^{-1} was due to sulfate groups $\nu(OSO_3H)$ and δ(OH) bending vibration of COOH. The peak at ≈1097 cm^{-1} was assigned to the ν(C–O) stretching vibration. The increased intensity of the O–H peak after oxidation and the appearance of C–H, C=O, C–O and OSO_3H bonds suggest that oxidation of the MWCNTs successfully introduced COOH, OH, C=O and OSO_3H groups onto the walls of the nanotubes [14,29,33]. The FTIR transmission spectrum of e-MWCNT (Fig. 1a) showed the absence of the band at ≈1726 cm^{-1} and the simultaneous appearance of a band at a lower frequency (≈1650 cm^{-1}), assigned to stretching of the amide carbonyl (C=O). In addition, the presence of new bands at ≈1580 and ≈1180 cm^{-1}, correspond to N–H in-plane and C–N bond stretching, respectively. The peaks at ≈3300–3600 cm^{-1} were due to the NH_2 stretch of the amine group. A band at ≈800 cm^{-1} was due to the out-of-plane NH_2 bending mode [22,29]. The FTIR results verify that amines were covalently attached to the MWCNTs. All of these groups introduced on surface of the MWCNTs can provide numerous sorption sites and thereby increase the sorption capacity of oxidized and amino-functionalized MWCNTs [12].

Thermogravimetric analysis, TGA, gave useful information about the functionalized MWCNTs, because most of the organic functional moieties on the MWCNTs were thermally unstable, *i.e.*, most of the organic functional groups were decomposed before the onset of MWCNTs weight loss (Fig. 1b). The pristine MWCNTs sample was stable and hardly decomposed below 800 °C while the o-MWCNT exhibited a weight loss of about 12 wt% (Fig. 1b). The thermal degradation of o-MWCNT and e-MWCNT was multistage processes due to the different functional groups introduced onto the surface of the nanotubes. The first weight loss interval below 200 °C of all the samples was attributed mainly to the evaporation of saturated water [30]. At higher temperatures, the weight loss can be attributed to the thermal decomposition of side-groups. Thus, according to the TG analysis, the amount of amine covalently bonded to the MWCNTs was estimated, based on the total weight of e-MWCNT, to be about 7 wt% in relation to the o-MWCNT. The attachment of amine at the surface of e-MWCNT was further confirmed by elemental analysis (Table 1). No nitrogen could be detected from the raw-MWCNT but a small amount of nitrogen (0.49%) was observed for o-MWCNT due to the oxidation. Based on the results presented in Table 1, the nitrogen content (4.08%) of e-MWCNT can also provide an estimation of the amount of attached amine (around 7 wt%), which is in accordance with the TGA results. Furthermore, the found decrease in the oxygen content of e-MWCNT (13.50%) in comparison to that of o-MWCNT (15.56%) may also provide direct evidence for the attachment of amines.

The physical properties of the raw-MWCNT, o-MWCNT and e-MWCNT are given in Table 2. It is evident that the surface area and pore volume of o-MWCNT were lower than those of the raw-MWCNT, while the average pore diameter was slightly increased after oxidation. This could be due the length of the o-MWCNT becoming shorter and the confined space among isolated MWCNTs appeared narrower after the raw-MWCNT had been oxidized. Furthermore, blockage of the pore entrances by the formation of oxygen-containing functional groups, which are direct products of oxidation, may also result in a decrease in the surface area of MWCNTs [13]. The surface area, average pore diameter and pore volume of o-MWCNT increased after EDA modification. This could be explained if the interparticle repulsions among e-MWCNT resulted in smaller-sized "globs" of MWCNT or if the additional ultrasound treatment used during amino-functionalization resulted in smaller aggregates of e-MWCNT.

The raw-MWCNTs have a pH_{PZC} of 4.98, while the o-MWCNT have a pH_{PZC} of 2.43 (Table 2). The decrease in the pH_{PZC} of the o-MWCNT compared to the raw-MWCNT is a result of the attachment of acidic oxygen-containing functional groups to the nanotube walls [14]. The amino groups on e-MWCNT show basic character and, thus, the pH_{PZC} of e-MWCNT (5.91) is higher than those of the raw-MWCNT and the o-MWCNT. From an electrostatic interaction point of view, sorption of Cd^{2+} onto MWCNT is favored at pH values greater than the pH_{PZC} as the surface of the MWCNT become more negatively charged. This was confirmed by zeta potential measurements at pH values higher than the pH_{PZC} of the samples and all samples showed negative values (Table 2).

The functional groups on the surfaces of raw-MWCNT, o-MWCNT and e-MWCNT were quantitatively measured by the Boehm method (Table 3). In the raw-MWCNT and o-MWCNT, lactonic groups dominated, followed by phenolic and carboxylic groups; similarly result was obtained in literature [13]. Concentrated sulfuric is strong dehydration agent, which could promote formation of lactonic groups [34]. Both the raw-MWCNT and o-MWCNT contained more total acidic sites than total basic sites, implying acidic characteristics of their surfaces. The o-MWCNT had 7 times more total surface acidic sites and 2.1 times more total surface basic sites than the raw-MWCNT. Surface modification of o-MWCNT by EDA was found to significantly raise the surface basicity of e-MWCNT, as a result of reaction of the carboxyl groups with EDA. Moreover, some lactones could react with amino groups forming amide and concomitantly phenol groups. The quantitative Kaiser test [35] predicted the concentration of terminal amino functions present on the e-MWCNT material to be 0.65 mmol g^{-1} of free amino groups per gram of e-MWCNT.

The dispersibility of MWCNTs in water was remarkably changed after modification (Fig. 2a–c). The pristine MWCNTs had a strong tendency to agglomerate due to their nano-size and high sur-

Table 2
Physical properties of raw-MWCNT, o-MWCNT and e-MWCNT.

Sorbents	Surface area (m^2 g^{-1})	Pore volume (cm^3 g^{-1})	Av. pore diameter (nm)	pH_{PZC}	Zeta potential (mV)
raw-MWCNT	187.58	0.755	16.09	4.98	−13.7 (pH 5.30)
o-MWCNT	78.49	0.328	16.72	2.43	−50.0 (pH 3.98)
e-MWCNT	101.24	0.538	21.25	5.91	−26.9 (pH 6.60)

Table 3
Results of the Boehm titrations.

	Carboxyls (mmol g^{-1})	Lactones (mmol g^{-1})	Phenols (mmol g^{-1})	Total acidic sites (mmol g^{-1})	Total basic sites (mmol g^{-1})
raw-MWCNT	0.066	0.279	0.235	0.584	0.197
o-MWCNT	0.87	1.78	1.43	4.09	0.415
e-MWCNT	0.15	1.24	1.83	3.22	1.15

Fig. 2. Dispersion of (a) raw-MWCNT, (b) o-MWCNT and (c) e-MWCNT in water at a concentration of 1 mg mL^{-1}.

face energy; thus poor dispersion in water was observed (Fig. 2a). However, oxidation introduces polar (hydrophilic) groups on the MWCNTs surface (Fig. 2b) and therefore, created the electrostatic stability required for a long time stable dispersion in water [29]. The dispersibility of the e-MWCNT was lower than that o-MWCNT due to possible hydrogen bond formation between the amine functionalities and interconnections between the nanotubes [29]. Good dispersibility of modified MWCNTs in water opens the path for their facile manipulation and processing in analytical chemistry and environmental protection.

For the practical employment of MWCNTs as sorbents in water and wastewater treatment, it is desirable that they are not cytotoxic because of possible life cycle interactions with animals and humans. The cytotoxicity induced by modified MWCNTs and the control raw-MWCNT was determined using L929 cells [29]. The results presented in Fig. 3a show that all samples of MWCNTs at the highest dose (100 μg mL^{-1}) time dependently decreased the number of L929 cells in cultures. However, only the raw-MWCNT but not the chemically modified MWCNTs impaired cell growth at a dose of 10 μg mL^{-1}. At the lowest examined dose (1 μg mL^{-1}) none of the MWCNT samples significantly modified the number of L929 cells in the culture [29]. The reduction of cell number could be a consequence of cell death. To verify this, the processes of cellular apoptosis and necrosis were examined. Neither the modified MWCNTs nor the raw-MWCNT were cytotoxic up to doses of 50 μg mL^{-1}. However, o-MWCNT and e-MWCNT induced apoptosis at the highest concentration (100 μg mL^{-1}) but the effect was relatively weak, since the percentage of apoptotic cells did not exceed 10% [29]. Another reason for a reduction of cell number in a culture could be inhibition of cellular proliferation. All the MWCNT samples dose dependently inhibited cellular proliferation. Lower doses (3–25 μg mL^{-1}) of modified MWCNTs were less inhibitory than the same doses of raw-MWCNT (Fig. 3b). A number of studies showed that pristine CNTs are cytotoxic and that the effect depends on the type of CNTs, mode of their preparation and cell types used for biocompatibility studies [25,26]. In contrast, functionalization significantly improves the dispersibility of CNTs in water and reduces their cytotoxicity [27–29], which was also shown in this study for e-MWCNTs. Although further studies are needed to confirm whether e-MWCNTs are biocompatible *in vivo*, the results obtained *in vitro* are very promising. As recommended by ISO 10993-5:2007, the cytotoxic test on fibroblast cell lines is the first screening assay for biocompatibility evaluation before using the *in vivo* assays.

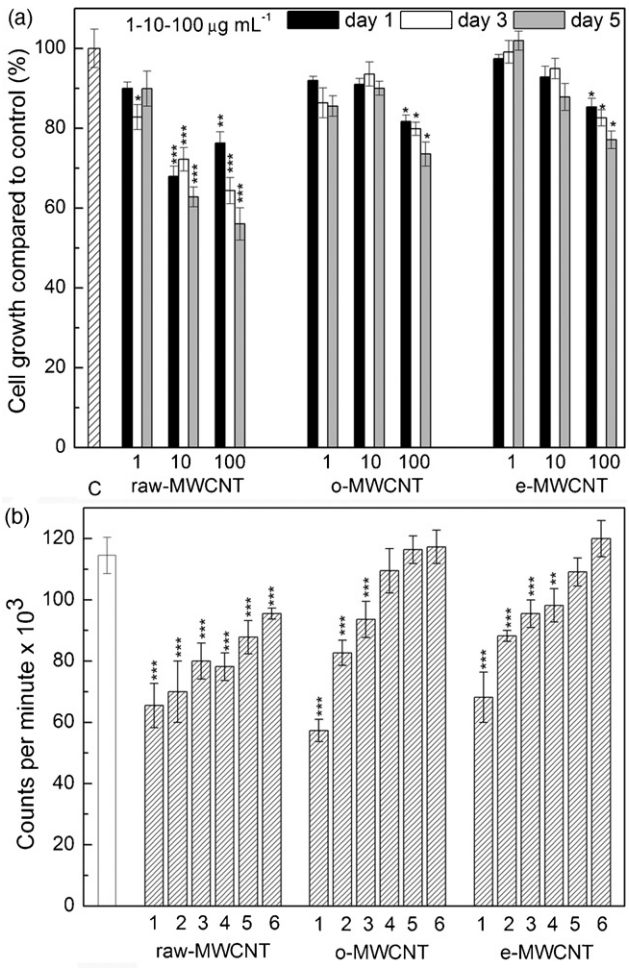

Fig. 3. (a) Effect of raw-MWCNT, o-MWCNT and e-MWCNT on L929 cell growth in cultures. The values are given as percentages of cell number ± SD (n = 4) compared to control of one representative experiment; (*p < 0.05; **p < 0.01; ***p < 0.005 compared to the control (one way ANOVA)), (b) Proliferation activity of L929 cells cultivated with different concentrations of MWCNTs. The values are given as mean cpm ± SD (triplicates); (*p < 0.05; **p < 0.01; ***p < 0.005 compared to the control (c) (Student t-test), 1 = 100 μg mL^{-1}; 2 = 50 μg mL^{-1}; 3 = 25 μg mL^{-1}; 4 = 12.5 μg mL^{-1}; 5 = 6.0 μg mL^{-1}; 6 = 3.0 μg mL^{-1}).

3.2. Adsorption studies

The adsorption behavior of Cd^{2+} on raw-MWCNT, o-MWCNT and e-MWCNT was investigated at pH values ranging from 2.0 to 11.0 (Fig. 4). Sorption of Cd^{2+} on o-MWCNT and e-MWCNT was strongly dependent on the pH value of the solution, since pH affects the surface charge of functionalized MWCNTs, the degree of ionization, metal speciation in aqueous solution and the surface properties of MWCNTs. It is known that cadmium species can be present in DI water in the forms of Cd^{2+}, $Cd(OH)^+$, $Cd(OH)_{2(s)}$, *etc.* [36]; at pH below 9, the dominant cadmium species is Cd^{2+} in the form of complex $[Cd(H_2O)_6]^{2+}$ [37].

It can be noticed that e-MWCNT show best sorption capacities in the pH range 8–9, and o-MWCNT in the pH range 6–10 (Fig. 4). However, Cd^{2+} sorption on raw-MWCNT was only slightly pH dependent. There was a noticeable, significant increase of Cd^{2+} sorption in the pH range 4–6 for o-MWCNT. A pH higher than 6 is beneficial for the ionization of the surface acidic groups, such as carboxylic groups (pKa 3–6), that play a significant role in the uptake of Cd^{2+} ions. The negative charges generated at the nanotube surface at pH > pH_{PZC} (2.43) enlarged the cation-exchange capacity of o-MWCNT and, simultaneously, the electrostatic attraction became

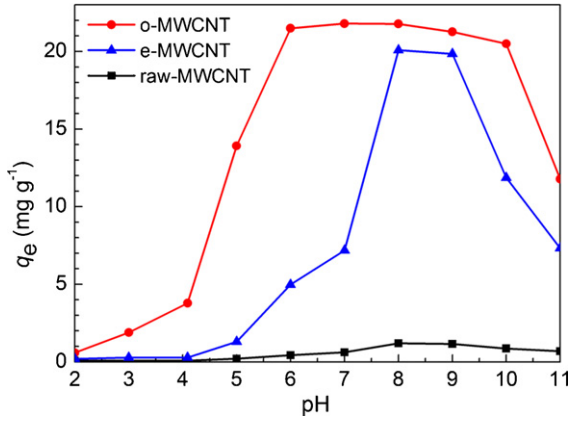

Fig. 4. Effect of pH on the adsorption of Cd^{2+} on raw-MWCNT, o-MWCNT and e-MWCNT. $C[Cd^{2+}]_0 = 5\,mg\,L^{-1}$, $m/V = 100\,mg\,L^{-1}$, $T = 25\,^{\circ}C$.

more important [13]. The removal efficiency at pH values lower than 4 was negligible due to the low dissociation of the carboxylic groups and competition between H^+ and Cd^{2+} ions for the same sorption site [12]. The amino group on e-MWCNT, having a pK_a value greater than 7 [23] and a pH_{PZC} 5.91, mainly contribute to the sorption of Cd^{2+}. A decrease of e-MWCNT adsorption capacity at pH values higher than 9.0 is in agreement with the decrease of the Cd^{2+} concentration and an increase of the concentration of ionic species, which have a lower affinity towards amino groups. Also, precipitation of $Cd(OH)_2$ at pH higher than 10 occupies sorption sites at both o-MWCNT and e-MWCNT, gradually preventing Cd^{2+} sorption as the pH increases. Precipitated $Cd(OH)_2$ was determined at particular pH values and subtracted from the overall available amount of Cd^{2+} ions; thus reliable values of the amounts of adsorbed Cd^{2+} were obtained.

The removal of Cd^{2+} ions from aqueous solution by raw-MWCNT, o-MWCNT and e-MWCNT as a function of contact time is presented in Fig. 5a. The adsorption onto all three types of MWCNTs increased very rapidly with contact time and 30 min were sufficient for the sorption equilibrium to be achieved. Since equilibrium of the adsorption process required only 30 min, the adsorption time was fixed at 45 min in subsequent adsorption experiments.

The adsorption kinetic models used in this study were a pseudo-first and pseudo-second-order rate equations [12]. Judging from the regression coefficients (r), Δq values and the calculated standard errors of the parameters for both models, the experimentally obtained kinetic data could be satisfactorily explained by a pseudo-second-order rate equation (Eq. (2)), showing good agreement of the q_e values (Table 4) with the results of experimental work (Figs. 4 and 5a). Separation of the variables in the differential form of the pseudo-second-order equation and integration gives:

$$\frac{t}{q_t} = \frac{1}{K' q_e^2} + \frac{1}{q_e} t \tag{2}$$

where q_e and q_t are the amounts of metal ion adsorbed ($mg\,g^{-1}$) at equilibrium and at time t, respectively. K' ($g\,mg^{-1}\,min^{-1}$) is the pseudo-second-order rate constant of adsorption.

The line plots of t/q_t versus t are presented in Fig. 5b, and values of q_e, K', r and Δq are listed in Table 4. Considering the values

Table 4
Kinetic parameters of the pseudo-second-order equation for Cd^{2+} adsorption on raw-MWCNT, o-MWCNT and e-MWCNT.

	q_e ($mg\,g^{-1}$)	K' ($g\,mg^{-1}\,min^{-1}$)	Δq (%)	r
raw-MWCNT	1.29 ± 0.04	0.135 ± 0.007	2.35	0.997
o-MWCNT	22.32 ± 0.21	0.0317 ± 0.0013	2.16	0.996
e-MWCNT	21.23 ± 0.18	0.0319 ± 0.0011	1.98	0.997

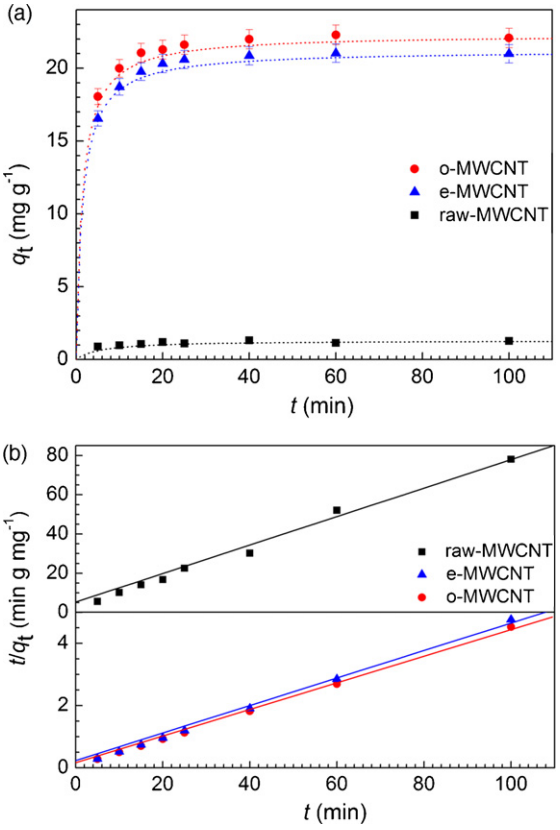

Fig. 5. (a) Effect of time on the sorption of Cd^{2+} by raw-MWCNT, o-MWCNT and e-MWCNT ($C[Cd^{2+}]_0 = 5\,mg\,L^{-1}$, $m/V = 100\,mg\,L^{-1}$, pH 8, $T = 25\,^{\circ}C$). Lines: Pseudo-second-order kinetics model. (b) Pseudo-second-order kinetics for the sorption of Cd^{2+} by raw-MWCNT, o-MWCNT and e-MWCNT. ($C[Cd^{2+}]_0 = 5\,mg\,L^{-1}$, $m/V = 100\,mg\,L^{-1}$, pH 8, $T = 25\,^{\circ}C$).

of K' constants, it could be concluded that faster equilibrium was achieved in the case of Cd^{2+} adsorption onto raw-MWCNTs. The slower adsorption rates on o-MWCNT and e-MWCNT indicate that processes with higher energetic barrier [12], such as chemisorption and/or surface complexation, are operative. The confirmation of pseudo-second-order kinetics, which is common for the removal of metals by carbonaceous materials [15], indicates the concentrations of both sorbate (Cd) and sorbent (raw-MWCNT, o-MWCNT and e-MWCNT) are involved in the rate determining step of the adsorption process [38].

Langmuir and Freundlich isotherms are used to model many adsorption processes. The Langmuir isotherm assumes a monolayer coverage of adsorbate over a homogeneous adsorbent surface and the adsorption of each molecule onto the surface has the same activation energy of adsorption. The Freundlich isotherm assumes a heterogeneous surface with a non-uniform distribution of heat of adsorption over the surface with the possibility of multilayer adsorption [21]. The adsorption isotherms of Cd^{2+} on raw-MWCNT, o-MWCNT and e-MWCNT at 25, 35 and 45 °C are presented in Fig. 6a. The equilibrium adsorption data can be correlated with the isotherm models of Langmuir (Eq. (3)) or Freundlich (Eq. (4)) [12]:

$$q = \frac{bq_{max}C}{1 + bC} \quad \text{or} \quad \frac{C}{q} = \frac{1}{bq_{max}} + \frac{C}{q_{max}} \tag{3}$$

$$q = k_f C^n \text{ or } \log q = \log k_f + n \log C \tag{4}$$

where C is the equilibrium concentration of metal ions remaining in the solution ($mol\,L^{-1}$); q is the amount of metal ions sorbed per weight unit of solid after equilibrium ($mol\,g^{-1}$); q_{max} and b are Langmuir constants related to the sorption capacity and sorption affinity, respectively. The maximum sorption capacity q_{max} is the

Table 5
Langmuir and Freundlich isotherm parameters for Cd^{2+} adsorption on raw-MWCNT, o-MWCNT and e-MWCNT.

T (°C)	Langmuir parameters				Freundlich parameters			
	q_{max} (mg g^{-1})	b (L mol^{-1})	Δq (%)	r	k_f (mol^{1-n} L^n g^{-1})	n	Δq (%)	r
raw-MWCNT								
25	1.26 ± 0.02	146,719 ± 4667	2.99	0.996	0.00227 ± 0.00017	0.524 ± 0.031	12.06	0.967
35	2.20 ± 0.03	156,550 ± 5177	3.76	0.997	0.00482 ± 0.00032	0.538 ± 0.034	15.58	0.960
45	3.19 ± 0.08	162,862 ± 6545	3.95	0.991	0.00710 ± 0.00049	0.539 ± 0.035	17.18	0.957
o-MWCNT								
25	22.39 ± 0.36	247,359 ± 9121	2.66	0.996	0.127 ± 0.009	0.601 ± 0.032	18.76	0.973
35	22.97 ± 0.31	289,532 ± 9462	3.30	0.997	0.122 ± 0.009	0.590 ± 0.036	19.05	0.967
45	24.15 ± 0.33	378,447 ± 14,741	3.66	0.997	0.113 ± 0.008	0.571 ± 0.037	20.67	0.960
e-MWCNT								
25	21.67 ± 0.40	243,516 ± 8440	2.34	0.995	0.123 ± 0.009	0.602 ± 0.033	18.57	0.969
35	23.28 ± 0.53	357,622 ± 13,946	3.26	0.992	0.096 ± 0.007	0.563 ± 0.038	20.07	0.963
45	25.70 ± 0.79	465,265 ± 20,143	4.14	0.996	0.078 ± 0.006	0.531 ± 0.034	19.87	0.968

amount of sorbate at complete monolayer coverage (mol g^{-1}), and b (L mol^{-1}) is a constant relating to the heat of sorption. The value of k_f (mol^{1-n} L^n g^{-1}) represents the sorption capacity when the equilibrium metal ion concentration equal 1 and n represents the degree of dependence of the sorption on the equilibrium concentration.

The Langmuir (Fig. 6b) and Freundlich constants were obtained by fitting the adsorption equilibrium data to the isotherm models; they are listed in Table 5. It can be noticed that the r values for the Langmuir model are higher, Δq values and calculated standard errors of the parameters are lower, than those of the Freundlich model, thus indicating that the Langmuir model better describes adsorption onto MWCNTs. For all three investigated types of MWCNTs, both q_{max} and b values increase with increasing temperature, while the standard errors of these parameters remain similar. Moreover, these values indicate that the best adsorption capacity for Cd^{2+} was achieved with e-MWCNT at increased temperatures, leading to the possible employment of functionalized MWCNTs for the removal of Cd^{2+} ions from industrial wastewater.

The Gibbs free energy (ΔG^0), enthalpy (ΔH^0) and entropy (ΔS^0) were calculated using the following Van't Hoff thermodynamic equations [19]:

$$\Delta G^0 = -RT\ \ln(b) \tag{5}$$

$$\ln(b) = \frac{\Delta S^0}{R} - \frac{\Delta H^0}{RT} \tag{6}$$

where T is the absolute temperature in K and R is the universal gas constant (8.314 J mol^{-1} K^{-1}). The Langmuir sorption constant b was derived from the isotherm experiments. ΔH^0 and ΔS^0 can be obtained from the slope and intercept of the linear plots of $\ln(b)$ *versus* T^{-1}, respectively (Fig. 7), assuming the sorption kinetics to be under steady-state conditions. The goodness of data fit was confirmed by the high r values and low standard errors of the estimated thermodynamic parameters (Table 6). The calculated thermodynamic values (Table 6) give some information concerning the sorption mechanism for the studied carbon nanotubes.

The negative values of ΔG^0 indicate that the adsorption of Cd^{2+} onto MWCNTs is a spontaneous process. It is noticeable that

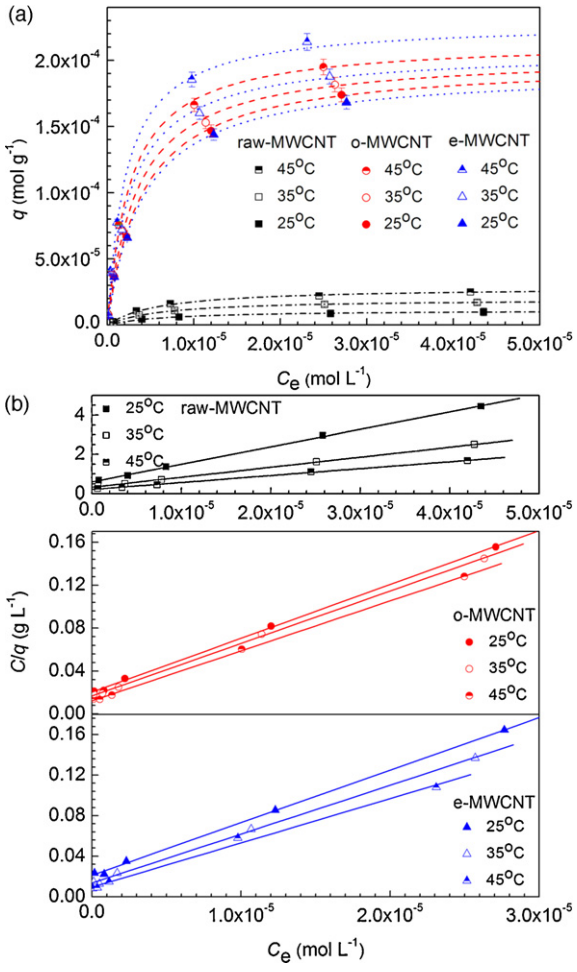

Fig. 6. (a) Adsorption isotherms of Cd^{2+} on the raw-MWCNT, o-MWCNT and e-MWCNT at 25, 35 and 45 °C. Lines: Langmuir model. (b) Langmuir isotherm for Cd^{2+} sorption on raw-MWCNT, o-MWCNT and e-MWCNT at 25, 35 and 45 °C. (m/V = 100 mg L^{-1}, pH 8).

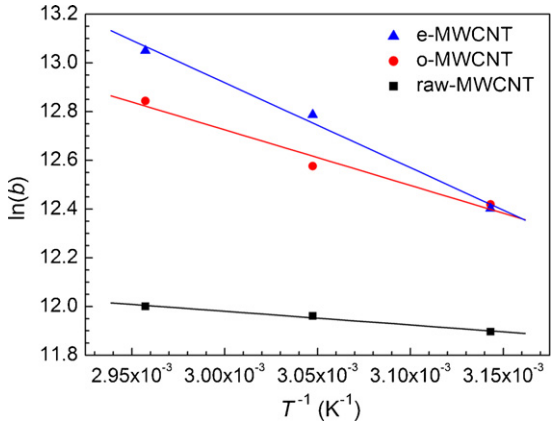

Fig. 7. Plot of $\ln(b)$ *versus* T^{-1} for the estimation of the thermodynamic parameters for the adsorption of Cd^{2+} ions onto raw-MWCNT, o-MWCNT and e-MWCNT.

Table 6
Thermodynamic parameters for Cd^{2+} adsorption onto raw-MWCNT, o-MWCNT and e-MWCNT.

T (°C)	Thermodynamic parameters			
	ΔG^0 (kJ mol^{-1})	ΔH^0 (kJ mol^{-1})	ΔS^0 (J mol^{-1} K^{-1})	r
raw-MWCNT				
25	−31.47 ± 0.19			
35	−32.63 ± 0.16	4.68 ± 0.12	113.64 ± 1.76	0.992
45	−33.74 ± 0.32			
o-MWCNT				
25	−32.85 ± 0.18			
35	−34.31 ± 0.17	18.96 ± 0.16	162.68 ± 7.27	0.987
45	−36.11 ± 0.21			
e-MWCNT				
25	−32.81 ± 0.21			
35	−34.89 ± 0.34	32.82 ± 0.18	206.29 ± 7.34	0.997
45	−36.69 ± 0.48			

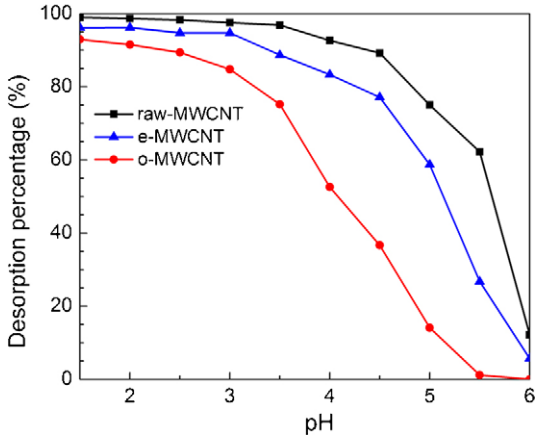

Fig. 8. Desorption of Cd^{2+} from raw-MWCNT, o-MWCNT and e-MWCNT at different pH values of the solution.

the ΔG^0 values decrease with increasing temperature, indicating that the process was more efficient at higher temperatures. The lowest ΔG^0 value was obtained in the case of Cd^{2+} adsorption on e-MWCNT at 45 °C. Regardless of coordination, at higher temperatures, solvated Cd^{2+} ions are readily desolvated, diffusion through the boundary layer and within the pores are faster processes and the adsorption processes become more favorable. The change in free energy for physisorption is generally between −20 and 0 kJ mol^{-1}, the physisorption together with chemisorption occur within the range −20 to −80 kJ mol^{-1} and chemisorption within the range −80 to −400 kJ mol^{-1} [19]. The calculated ΔG^0 values suggest that the interaction between Cd^{2+} and e-MWCNT, as well as the interactions between Cd^{2+} and raw-MWCNT and o-MWCNT, can be considered as resulting from contributions of both physisorption and chemisorption processes.

The positive values of ΔH^0 show that Cd^{2+} adsorption onto the studied MWCNTs are endothermic processes. One of the possible interpretation of endothermicity is that the ion $[Cd(H_2O)_6]^{2+}$ needs energy to break off the hydration shell and to be accessible for interaction with the surface of MWCNT. The removal of water molecules from the $[Cd(H_2O)_6]^{2+}$ ions is an endothermic process and according to the ΔH^0 value of the overall adsorption process, the endothermicity of the desolvation process significantly exceeded the enthalpy of adsorption. It is generally accepted that physical sorption involves an enthalpy change between 2 and 21 kJ mol^{-1}, while the enthalpy change of chemisorption falls within the range 80–200 kJ mol^{-1} [39]. From this point of view, the adsorptions of Cd^{2+} onto raw-MWCNT and o-MWCNT were mainly physisorption processes, while both physisorption and chemisorption contribute to the adsorption of Cd^{2+} ions onto e-MWCNT. The positive values of ΔS^0 indicate a tendency to higher disorder at the interface between the MWCNT and Cd^{2+} solutions. The fixation of Cd^{2+} ions resulted in a decrease in the freedom of the whole system. However, in some processes, such as ion exchange, ions from the solid surface are released into the bulk solution, which results in an increase of the overall entropy of the system.

Repeated availability is an important factor for an advanced adsorbent. Such an adsorbent not only possesses a high adsorption capability, but also exhibits good desorption properties, which significantly reduce the overall cost for the adsorbent. The percentage desorption of Cd^{2+} ions into solutions of various pH values is shown in Fig. 8. It is apparent that Cd^{2+} desorption increased with decreasing pH. About 1.5% of Cd^{2+} was desorbed from o-MWCNT at pH 5.5; this increased sharply at pH < 5.5 and reached a value of about 93% at pH 1.5. The e-MWCNT and raw-MWCNT showed a higher desorption of Cd^{2+} at pH < 6 and reached 96% and 99% at pH 1.5, respectively. These results show that the Cd^{2+} adsorbed by e-MWCNT could be more easily desorbed than that adsorbed on o-MWCNT, suggesting a weaker binding between e-MWCNT and Cd^{2+}, which means that e-MWCNT can be repeatedly employed in heavy metal wastewater management.

The maximum adsorption capacity of the MWCNTs increased in the temperature range 25–45 °C, indicating a complex sorption processes and changes in the contributions of individual sorption mechanisms to the overall process: the co-existence of physisorption, *i.e.*, ion exchange, electrostatic attraction and chemisorption, *i.e.*, surface complexation. Raw-MWCNT behaves as a weak proton acceptor, releasing hydroxide ions and increasing slightly the pH of the solution, presented by the following reaction (7) [40]:

$$MWCNT_\pi + H_2O \rightleftharpoons MWCNT_\pi\text{-}H^+ + OH^- \quad (7)$$

Analogously, Cd^{2+} adsorption on raw-MWCNT might occur through interactions between the π electrons of the basal planes (π-electron densities of the graphene structure) of the carbon nanotubes and Cd^{2+} ions, according to reaction (8) [40]:

$$2(MWCNT_\pi\text{-}H^+) + Cd^{2+} \rightleftharpoons (MWCNT_\pi)_2\text{-}Cd^{2+} + 2H^+ \quad (8)$$

The pH of the residual solution after Cd^{2+} adsorption showed a slight decrease, corroborating the presented mechanism (8) and indicating a main contribution of reaction (8) to overall adsorption process. The fast equilibration process for the raw-MWCNT, according to the kinetic data, could be understood in the sense of probably weak ion-π electron densities interactions of a lower energetic barrier.

In this and in a previous study [8], it was found that the metal ion sorption capacity of o-MWCNT was not in direct correlation with their specific surface area, pore specific volume and mean pore diameter but strongly depended on their total surface acidity. The metal ion sorption capacity of MWCNTs increased with increasing total surface acidity, including carboxyls, lactones and phenols, present on the surface sites of MWCNTs. It was concluded that the sorption of Cd^{2+} onto o-MWCNT was a chemisorption process rather than a physisorption process [8]. Analogously, the higher sorption capacity of o-MWCNT compared to raw-MWCNT indicates the highest contribution of the introduced oxygen-containing groups, which also indicates that chemisorption was the more probable process. Moreover, acidic oxygen-containing groups might behave as ion-exchange sites for the retention of Cd^{2+} cations, giving rise to the formation of metal ligand surface complexes [40]. The binding of Cd^{2+} onto the surface of o-MWCNT having polar functional groups (P) (COOH, C=O, OSO_3H and OH) could be described as [38]:

$$Cd^{2+} + 2(MWCNT\text{-}P^-) \rightleftharpoons Cd(MWCNT\text{-}P)_2 \quad (9)$$

or

$$Cd^{2+} + 2(MWCNT\text{-}HP) \rightleftharpoons Cd(MWCNT\text{-}P)_2 + 2H^+ \quad (10)$$

or *via* the formation of cadmium complexes and hydrogen bonding between the surface functional groups and hydrated cadmium cations [40–42]. Jia and Thomas [41] presented possible modes of carboxylate and phenolic coordination with cadmium cation where carboxyl groups have a key role for Cd^{2+} adsorption on the o-MWCNT. Also, a moderate contribution of OSO_3H functional group (soft Lewis base), which shows high coordination capacity with heavy metal such as Cd^{2+} ions (soft Lewis acid), should not be neglected [33,38]. In relation to the proposed adsorption mechanism (10), a greater decrease of initial pH of o-MWCNT and e-MWCNTs solutions, in comparison to raw-MWCNT, was observed. Sorption processes, presented by Eqs. (9) and (10), were also operative for the raw-MWCNT but of lower significance than those given by Eqs. (7) and (8) [40].

At the surface of e-MWCNT, free amino and non-reacted oxygen-containing functional groups were present. Hence, besides the presented adsorption mechanisms for o-MWCNT, additional coordination and electrostatic interactions are possible between Cd^{2+} ions and unprotonated amino groups at pH values higher than 7:

$$MWCNT\text{-}CONH(CH_2)_2NH_2 + Cd^{2+} \rightleftharpoons Cd[MWCNT\text{-}CONH(CH_2)_2NH_2]^{2+} \quad (11)$$

Also, amino groups on the MWCNT surface could be involved in the chelation interactions during the adsorption process [19–22].

The q_{max} and b values of the e-MWCNT were compared with the metal adsorption capacities reported in the literature for other adsorbents (Table 7), although a direct comparison between the examined modified MWCNT with those obtained in literature was difficult, due to the varying experimental conditions employed in those studies. However, it may be seen that the q_{max} and b values differ widely for different adsorbents (Table 7). More generally, the metal removal capacity of e-MWCNT was higher than that of ash, zeolite, silica and bacterium, most carbon nanotubes and agricultural wastes, as well as of some carbons, biomasses and algae. Significantly higher capacities were shown by commercial resins, some carbons and biomasses. Comparison of q_{max} values showed that the e-MWCNT sample exhibited a reasonable capacity for Cd^{2+} adsorption from aqueous solutions. It is well known that not only sorption capacity, but also sorption affinity is important. If the main objective of a sorption technology in practice is to be economic concerning the amount of adsorbent consumed and the requirements concerning water purity are moderate, the adsorption facility will be operated up to near saturation of the adsorbent and hence sorption capacity is of crucial importance. If extreme water purity is the goal, the facility will be operated "at the left side of the adsorption isotherm" and the sorption affinity is the most important criterion. Comparison of the b values showed that the e-MWCNT exhibits excellent affinity for Cd^{2+} adsorption from aqueous solutions (Table 7).

The cost of adsorbents is also an important parameter for their employment in adsorption processes. Given the current cost of MWCNTs (≈50 $/g) [65], they are unlikely to replace activated carbons (≈0.08 $/g) [66] soon in large-scale engineering applications designed for the treatment and removal of Cd^{2+} contaminants by adsorption. Synthetic resins are used because they are very effective and provide some selectivity toward certain metals. However, they are very costly with bulk prices ranging from 3 to 25 $/kg [52]. Agricultural wastes have several advantages over commercial resins in that they are less expensive (100 $/t [55]), biodegradable and come from renewable resources.

Practically every manufacturer currently uses catalytic CVD to make their tubes. Improved manufacture and large-scale production have already caused the price of CVD-produced CNTs to fall substantially, from around 200 $/g in 1999 to 2–50 $/g today [46,65]. Although there are other methods for producing CNTs, such as arc discharge and laser ablation, they do not produce CNTs in such large quantities as CVD. Hence, most current manufacturers are concentrating on the development of more efficient versions of CVD, as well as gaining more control over the types of tubes they make. Single-walled technology just has not taken off because of the cost. If the cost and price of carbon nanotubes decrease over the next few years then this will open up new opportunities for the product. CVD is deemed to be a promising route to reduce the cost of CNTs in the future, which would increase the use of CNTs in environmental protection applications. In addition, the practical use of

Table 7
Literature results of the adsorption of Cd^{2+} ions by various adsorbent.

Adsorbent	q_{max} (mg g^{-1})	b (L mol^{-1})	References
Carbon nanotubes			
CNT (HNO_3)	2.92	1,180,000	[14]
Nitrogen-doped MWCNT (HNO_3)	31		[43]
Cup-stacked MWCNT (HNO_3)	20	–	
CNT grown on microsized Al_2O_3 particles	8.89	14,613	[44]
CNT ($KMnO_4$)	11.0	–	[45]
MWCNT (HNO_3)	10.86	32,598.9	[46]
MWCNT (HNO_3)	7.42	–	[47]
Carbon			
Unmodified carbon	207.3	–	[31]
Triton X-100-modified carbon	232.9	–	
Oxidized granular activated carbon	5.74	31,860	[48]
Commercial activated carbon	4.29	11,061	[49]
Ash			
Rice husk ash	3.03	21,014	[50]
Biomass			
Cystine-modified biomass	11.63	170,863	[21]
Biomass grafted with polyamic acid	95.2	1,829,727	[22]
Agricultural waste			
Peanut hulls	6	–	[51]
Phosphoric acid modified corncob	52.8	–	[52]
Natural corncob	5.38	105,665.4	[53]
Citric acid oxidized corncob	55.7	219,199.5	
Nitric acid oxidized corncob	19.3	64,073.7	
Native starch	8.9	1.24	[54]
Oxidized starch	14.6	4.72	
Sugar beet pulp	24.39	6920	[55]
Algae			
Pelvetia caniculata	75	8430.7	[56]
Caulerpa lentillifera	4.70	8346.1	[57]
Aquatic moss			
Fontinalis antipyretica	28	14,613.3	[58]
Bacterium			
Sphaerotilus natans	45	1124.1	[59]
Inorganic			
Nano-B_2O_3/TiO_2 composite	49.9	786.8	[60]
Silica			
Amino-functionalized silica	18.25	28,395	[61]
Zeolite			
HEU-type zeolite	12.2	–	[62]
Resin			
Thio chelating resins	78.7	2800	[63]
Chelating resins containing N,N donor sets	16.64	–	[64]
Commercial resins			
Duolite GT-73	105.7	–	[51]
Amberlite IRC-718	258.5	–	
Lewatit TP 207	50	–	[53]
e-MWCNT	25.7	465,265	This study

CNTs as sorbents in water and wastewater treatment depends on continuation of research into the toxicity of CNTs and CNT-related materials.

The extraordinarily fast transport of water in CNTs could be utilized for the production of high-flux nanotube-based filtration membranes, in which aligned nanotubes serve as pores in an impermeable support matrix, in contrast to other materials, such as polymer membranes, with significantly lower fluxes [67]. Chemical functionalization at the entrance to CNT cores affects the selectivity of chemical transport across an aligned membrane structure [68]. Novel membranes drawing on the unique properties of CNTs may reduce significantly the energy and cost of desalination [69].

4. Conclusions

Amino-functionalization of MWCNTs by EDA using N-HATU significantly shortens the reaction time compared to the commonly employed acylation-amidation, which often takes several days. FTIR, TGA and elemental analysis results on samples at different stages of the functionalization process confirmed the modification process. Functionalized MWCNTs are of acceptable biocompatibility *in vitro* since they are not cytotoxic even at high concentrations ($50\,\mu g\,mL^{-1}$). Moreover, this material presents an appropriate adsorbent for the removal of Cd^{2+} ions from aqueous solutions.

The adsorption properties of raw-MWCNT were greatly improved by oxidation, as well as by amino-functionalization. It was found that the adsorption capacities change with increasing temperature, whereby the amino-functionalized MWCNT had the best adsorption capacity for Cd^{2+}. This gives the possibility that functionalized MWCNTs could be used for the production of filtration membranes for the removal of heavy metals from industrial waters at higher temperatures, and for preconcentration of heavy metals in analytical chemistry and environmental protection.

The kinetic data of the sorption on all the investigated MWCNTs were well fitted with the pseudo-second-order kinetic model, suggesting that the rate-limiting step was chemical sorption rather than diffusion.

The sorption of cadmium onto the studied MWCNTs is a rather complex process, the mechanism of which may include both of physisorption and chemisorption mechanisms. The metal ion sorption capacity and affinity of MWCNTs (raw and modified) strongly depended more on their surface groups, pH and temperature than on their surface area, pore volume and pore diameter.

The ICP-MS method applied in this study is advantageous because of its sensitivity which allowed the utilization of less concentrated sample solutions, thereby eliminating the need for large volume of Cd solution and large MWCNTs amounts and minimizing negative influences to the environment during the experimental study.

Acknowledgement

The authors are grateful to the Ministry of Science and Technological Development of the Republic of Serbia, Project Nos. 142006 and 142002 for financial support.

References

[1] S. Iijima, Helical microtubules of graphitic carbon, Nature 354 (1991) 56–58.
[2] L.M. Dai, A.W.H. Mau, Controlled synthesis and modification of carbon nanotubes and C60: carbon nanostructures for advanced polymeric composite materials, Adv. Mater. 13 (2001) 899–913.
[3] S.M. Lee, Y.H. Lee, Hydrogen storage in single-walled carbon nanotubes, Appl. Phys. Lett. 76 (2000) 2877–2879.
[4] G.L. Che, B.B. Lakshmi, E.R. Fisher, C.R. Martin, Carbon nanotubule membranes for electrochemical energy storage and production, Nature 393 (1998) 346–349.
[5] P.G. Collins, K. Bradley, M. Ishigami, A. Zettl, Extreme oxygen sensitivity of electronic properties of carbon nanotubes, Science 287 (2000) 1801–1804.
[6] P.G. Collins, A. Zettl, H. Bando, A. Thess, R.E. Smalley, Nanotube nanodevice, Science 278 (1997) 100–102.
[7] M. Valcárcel, S. Cárdenas, B.M. Simonet, Role of carbon nanotubes in analytical science, Anal. Chem. 79 (2007) 4788–4797.
[8] G.P. Rao, C. Lu, F. Su, Sorption of divalent metal ions from aqueous solution by carbon nanotubes: a review, Sep. Purif. Technol. 58 (2007) 224–231.
[9] K. Yang, W. Wu, Q. Jing, L. Zhu, Aqueous adsorption of aniline, phenol, and their substitutes by multi-walled carbon nanotubes, Environ. Sci. Technol. 42 (2008) 7931–7936.
[10] H. Katsumata, T. Matsumoto, S. Kaneco, T. Suzuki, K. Ohta, Preconcentration of diazinon using multiwalled carbon nanotubes as solid-phase extraction adsorbents, Microchem. J. 88 (2008) 82–86.
[11] Y. Liu, Y. Li, X.P. Yan, Preparation, Characterization, and application of L-cysteine functionalized multiwalled carbon nanotubes as a selective sorbent for separation and preconcentration of heavy metals, Adv. Funct. Mater. 18 (2008) 1536–1543.
[12] D. Xu, X. Tan, C. Chen, X. Wang, Removal of Pb(II) from aqueous solution by oxidized multiwalled carbon nanotubes, J. Hazard. Mater. 154 (2008) 407–416.
[13] C. Lu, C. Liu, Removal of nickel(II) from aqueous solution by carbon nanotubes, J. Chem. Technol. Biotechnol. 81 (2006) 1932–1940.
[14] Z. Gao, T.J. Bandosz, Z. Zhao, M. Han, J. Qiu, Investigation of factors affecting adsorption of transition metals on oxidized carbon nanotubes, J. Hazard. Mater. 167 (2009) 357–365.
[15] Z. Gao, T.J. Bandosz, Z. Zhao, M. Han, C. Liang, J. Qiu, Investigation of the role of surface chemistry and accessibility of cadmium adsorption sites on open-surface carbonaceous materials, Langmuir 24 (2008) 11701–11710.
[16] C. Lu, H. Chiu, Chemical modification of multiwalled carbon nanotubes for sorption of Zn^{2+} from aqueous solution, Chem. Eng. J. 139 (2008) 462–468.
[17] S. Banerjee, T. Hemraj-Benny, S.S. Wong, Covalent surface chemistry of single-walled carbon nanotubes, Adv. Mater. 17 (2005) 17–29.
[18] D. Tasis, N. Tagmatarchis, A. Bianco, M. Prato, Chemistry of carbon nanotubes, Chem. Rev. 106 (2006) 1105–1136.
[19] C.C. Liu, M. Kuang-Wang, Y.S. Li, Removal of nickel from aqueous solution using wine processing waste sludge, Ind. Eng. Chem. Res. 44 (2005) 1438–1445.
[20] S. Deng, Y.P. Ting, Characterization of PEI-modified biomass and biosorption of Cu(II), Pb(II) and Ni(II), Water Res. 39 (2005) 2167–2177.
[21] J. Yu, M. Tong, X. Sun, B. Li, Cystine-modified biomass for Cd(II) and Pb(II) biosorption, J. Hazard. Mater. 143 (2007) 277–284.
[22] J. Yu, M. Tong, X. Sun, B. Li, Biomass grafted with polyamic acid for enhancement of cadmium(II) and lead(II) biosorption, React. Funct. Polym. 67 (2007) 564–572.
[23] H.F. Gorgulho, J.P. Mesquita, F. Gonçalves, M.F.R. Pereira, J.L. Figueiredo, Characterization of the surface chemistry of carbon materials by potentiometric titrations and temperature-programmed desorption, Carbon 46 (2008) 1544–1555.
[24] I. Nicoletti, G. Migliorati, M.C. Pagliacci, F. Grignani, C. Riccardi, A rapid and simple method for measuring thymocyte apoptosis by propidium iodide staining and flow cytometry, J. Immunol. Methods 139 (1991) 271–279.
[25] S.K. Smart, A.I. Cassady, G.Q. Lu, D.J. Martin, The biocompatibility of carbon nanotubes, Carbon 44 (2006) 1034–1047.
[26] L. Zhu, D.W. Chang, L. Dai, Y. Hong, DNA damage induced by multiwalled carbon nanotubes in mouse embryonic stem cells, Nano Lett. 7 (2007) 3592–3597.
[27] H. Dumortier, S. Lacotte, G. Pastorin, R. Marega, W. Wu, D. Bonifazi, J.P. Briand, M. Prato, S. Muller, A. Bianco, Functionalized carbon nanotubes are non-cytotoxic and preserve the functionality of primary immune cells, Nano Lett. 6 (2006) 1522–1528.
[28] S. Lacotte, A. García, M. Dècossas, W.T. Al-Jamal, S. Li, K. Kostarelos, S. Muller, M. Prato, H. Dumortier, A. Bianco, Interfacing functionalized carbon nanohorns with primary phagocytic cells, Adv. Mater. 20 (2008) 2421–2426.
[29] G. Vuković, A. Marinković, M. Obradović, V. Radmilović, M. Čolić, R. Aleksić, P.S. Uskoković, Synthesis, characterization and cytotoxicity of surface amino-functionalized water-dispersible multi-walled carbon nanotubes, Appl. Surf. Sci. 255 (2009) 8067–8075.
[30] J. Xu, P. Yao, X. Li, F. He, Synthesis and characterization of water-soluble and conducting sulfonated polyaniline/*para*-phenylenediamine-functionalized multi-walled carbon nanotubes nano-composite, Mater. Sci. Eng. B 151 (2008) 210–219.
[31] M. Nadeem, M. Shabbir, M.A. Abdullah, S.S. Shah, G. McKay, Sorption of cadmium from aqueous solution by surfactant-modified carbon adsorbents, Chem. Eng. J. 148 (2009) 365–370.
[32] H.P. Boehm, Some aspects of the surface chemistry of carbon blacks and other carbons, Carbon 32 (1994) 759–769.
[33] R. Yu, L. Chen, Q. Liu, J. Lin, K.L. Tan, S.C. Ng, H.S.O. Chan, G.Q. Xu, T.S.A. Hor, Platinum deposition on carbon nanotubes via chemical modification, Chem. Mater. 10 (1998) 718–722.
[34] J.G. Coroneus, B.R. Goldsmith, J.A. Lamboy, A.A. Kane, P.G. Collins, G.A. Weiss, Mechanism-guided improvements to the single molecule oxidation of carbon nanotube sidewalls, Chem. Phys. Chem. 9 (2008) 1053–1056.
[35] V.K. Sarin, S.B.H. Kent, J.P. Tam, R.B. Merrifield, Quantitative monitoring of solid-phase peptide synthesis by the ninhydrin reaction, Anal. Biochem. 117 (1981) 147–157.
[36] R. Leyva-Ramos, J.R. Rangel-Mendez, J. Mendoza-Barron, L. Fuentes-Rubio, R.M. Guerrero-Coronado, Adsorption of cadmium(II) from aqueous solution onto activated carbon, Wat. Sci. Technol. 35 (1997) 205–211.

[37] K. Ozutsumi, T. Takamuku, S. Ishiguro, H. Ohtaki, An X-ray diffraction study on the structure of solvated cadmium(II) ion and tetrathiocyanatocadmate(II) complex in N,N-dimethylformamide, Bull. Chem. Soc. Jpn 62 (1989) 1875–1879.
[38] M.M. Rao, G.P.C. Rao, K. Seshaiah, N.V. Choudary, M.C. Wang, Activated carbon from *Ceiba pentandra* hulls, an agricultural waste, as an adsorbent in the removal of lead and zinc from aqueous solutions, Waste Manage. 28 (2008) 849–858.
[39] Y. Liu, Y.J. Liu, Biosorption isotherms, kinetics and thermodynamics, Sep. Purif. Technol. 61 (2008) 229–242.
[40] J. Jaramillo, V. Gómez-Serrano, P.M. Álvareza, Enhanced adsorption of metal ions onto functionalized granular activated carbons prepared from cherry stones, J. Hazard. Mater. 161 (2009) 670–676.
[41] Y.F. Jia, K.M. Thomas, Adsorption of cadmium ions on oxygen surface sites in activated carbon, Langmuir 16 (2000) 1114–1122.
[42] V. Strelko, D.J. Malik, Characterization and metal sorptive properties of oxidized active carbon, J. Colloid Interface Sci. 250 (2002) 213–220.
[43] G. Andrade-Espinosa, M. Emilio Muñoz-Sandoval, M. Terrones, H. Endo, J.R. Terrones, Rangel-Mendez, Acid modified bamboo-type carbon nanotubes and cup-stacked-type carbon nanofibres as adsorbent materials: cadmium removal from aqueous solution, J. Chem. Technol. Biotechnol. 84 (2009) 519–524.
[44] S.H. Hsieh, J.J. Horng, Adsorption behavior of heavy metal ions by carbon nanotubes grown on microsized Al_2O_3 particles, J. Univ. Sci. Technol. Beijing 14 (2007) 77–84.
[45] Y.H. Li, S. Wang, Z. Luan, J. Ding, C. Xu, D. Wu, A dsorption of cadmium(II) from aqueous solution by surface oxidized carbon nanotubes, Carbon 41 (2003) 1057–1062.
[46] Y.H. Li, J. Ding, Z. Luan, Z. Di, Y. Zhu, C. Xu, D. Wu, B. Wei, Competitive adsorption of Pb^{2+}, Cu^{2+} and Cd^{2+} ions from aqueous solutions by multiwalled carbon nanotubes, Carbon 41 (2003) 2787–2792.
[47] P. Liang, Y. Liu, L. Guo, J. Zeng, H. Lu, Multiwalled carbon nanotubes as solid-phase extraction adsorbent for the preconcentration of trace metal ions and their determination by inductively coupled plasma atomic emission spectrometry, J. Anal. At. Spectrom. 19 (2004) 1489–1492.
[48] X. Huang, N. Gao, Q. Zhang, Thermodynamics and kinetics of cadmium adsorption onto oxidized granular activated carbon, J. Environ. Sci. 19 (2007) 1287–1292.
[49] N. Kannan, G. Rengasamy, Comparison of cadmium ion adsorption on various activated carbons, Water Air Soil Pollut. 163 (2005) 185–201.
[50] V.C. Srivastava, I.D. Mall, I.M. Mishra, Competitive adsorption of cadmium(II) and nickel(II) metal ions from aqueous solution onto rice husk ash, Chem. Eng. Process. 48 (2009) 370–379.
[51] P. Brown, I.A. Jefcoat, D. Parrish, S. Gill, E. Graham, Evaluation of the adsorptive capacity of peanut hull pellets for heavy metals in solution, Adv. Environ. Res. 4 (2000) 19–29.
[52] T. Vaughan, C.W. Seo, W.E. Marshall, Removal of selected metal ions from aqueous solution using modified corncobs, Bioresour. Technol. 78 (2001) 133–139.
[53] R. Leyva-Ramos, L.A. Bernal-Jacome, I. Acosta-Rodriguez, Adsorption of cadmium(II) from aqueous solution on natural and oxidized corncob, Sep. Purif. Technol. 45 (2005) 41–49.
[54] D.K. Kweon, J.K. Choi, E.K. Kim, S.T. Lim, Adsorption of divalent metal ions by succinylated and oxidized corn starches, Carbohydr. Polym. 46 (2001) 171–177.
[55] Z. Reddad, C. Gerente, Y. Andresp, P. Le Ecloirec, Adsorption of several metal ions onto a low-cost biosorbent: kinetic and equilibrium studies, Environ. Sci. Technol. 36 (2002) 2067–2073.
[56] P. Lodeiro, B. Cordero, J.L. Barriada, R. Herrero, M.E. Sastre de Vicente, Biosorption of cadmium by biomass of brown marine macroalgae, Bioresour. Technol. 96 (2005) 1796–1803.
[57] P. Pavasant, R. Apiratikul, V. Sungkhum, P. Suthiparinyanont, S. Wattanachira, T.F. Marhaba, Biosorption of Cu^{2+}, Cd^{2+}, Pb^{2+}, and Zn^{2+} using dried marine green macroalga *Caulerpa lentillifera*, Bioresour. Technol. 97 (2006) 2321–2329.
[58] R.J.E. Martins, R. Pardo, R.A.R. Boaventura, Cadmium(II) and zinc(II) adsorption by the aquatic moss *Fontinalis antipyretica*: effect of temperature, pH and water hardness, Water Res. 38 (2004) 693–699.
[59] A. Esposito, F. Pagnanelli, A. Lodi, C. Solisio, F. Vegliò, Biosorption of heavy metals by *Sphaerotilus natans*: an equilibrium study at different pH and biomass concentrations, Hydrometallurgy 60 (2001) 129–141.
[60] O.M. Kalfa, Ö. Yalçinkaya, A.R. Türker, Synthesis of nano B_2O_3/TiO_2 composite material as a new solid phase extractor and its application to preconcentration and separation of cadmium, J. Hazard. Mater. 166 (2009) 455–461.
[61] A. Heidari, H. Younesi, Z. Mehraban, Removal of Ni(II), Cd(II), and Pb(II) from a ternary aqueous solution by amino functionalized mesoporous and nano mesoporous silica, Chem. Eng. J. 153 (2009) 70–79.
[62] V. Arámbula-Villazana, M. Solache-Ríos, M.T. Olgíun, Sorption of cadmium from aqueous solutions at different temperatures by Mexican HEU-type zeolite rich tuff, J. Incl. Phenom. Macrocycl. Chem. 55 (2006) 237–245.
[63] A.A. Atia, A.M. Donia, A.M. Yousif, Synthesis of amine and thio chelating resins and study of their interaction with zinc(II), cadmium(II) and mercury(II) ions in their aqueous solutions, React. Funct. Polym. 56 (2003) 75–82.
[64] S. Pramanik, S. Dhara, S.S. Bhattacharyya, P. Chattopadhyay, Separation and determination of some metal ions on new chelating resins containing N, N donor sets, Anal. Chim. Acta 556 (2006) 430–437.
[65] http://www.rsc.org/chemistryworld/Issues/2007/November/ManufacturingCarbonNanotubeMarket.asp.
[66] H.H. Cho, B.A. Smith, J.D. Wnuk, D.H. Fairbrother, W.P. Ball, Influence of surface oxides on the adsorption of naphthalene onto multiwalled carbon nanotubes, Environ. Sci. Technol. 42 (2008) 2899–2905.
[67] S. Joseph, N.R. Aluru, Why are carbon nanotubes fast transporters of water? Nano Lett. 8 (2008) 452–458.
[68] M. Majumder, N. Chopra, B.J. Hinds, Effect of tip functionalization on transport through vertically oriented carbon nanotube membranes, J. Am. Chem. Soc. 127 (2005) 9062–9070.
[69] M.S. Mauter, M. Elimelech, Environmental applications of carbon-based nanomaterials, Environ. Sci. Technol. 42 (2008) 5843–5859.